ELSEVIER

Ceramics International 26 (2000) 589–592

CERAMICS INTERNATIONAL

Czochralski growth and laser parameters of RE^{3+}-doped Y_2O_3 and Sc_2O_3

L. Fornasiero, E. Mix, V. Peters, K. Petermann*, G. Huber

Institut für Laser-Physik, Universität Hamburg, Jungiusstr. 9a, 20355 Hamburg, Germany

Received 8 July 1999; received in revised form 7 September 1999; accepted 4 October 1999

Abstract

Yttria exhibits a thermal conductivity which is higher than that of $Y_3Al_5O_{12}$. Moreover, it can be doped with rare earth ions. The isostructural scandia has similar characteristics. Due to these properties both oxides are attractive hosts for high power solid state lasers. We have grown yttrium oxide and scandium oxide crystals from rhenium crucibles by the Czochralski technique. The size of the crystals is limited because of problems to control the crystal diameter during the growth process. However, the grown rare earth doped samples show promising spectroscopic features. We report on the spectroscopic characteristics of Y_2O_3 and Sc_2O_3 doped with Ho^{3+}- and Er^{3+}-ions. Laser operation of Er:Sc_2O_3 near 3 μm wavelength has already been demonstrated.

Keywords: B. Spectroscopy; C. Optical properties; C. Thermal conductivity; DY_2O_3; Sc_2O_3

1. Introduction

The sesquioxide Y_2O_3 (yttria) has been investigated since the early sixties. Y_2O_3 has the bixbyite structure and belongs to the cubic space group Ia3 [1] with a lattice constant of 10.6 Å. The unit cell contains 16 formula units: 24 of the 32 cations in the unit cell reside on sites with C_2 point symmetry and eight on sites with C_{3i} point symmetry. The measured thermal conductivity of undoped Y_2O_3 is 14 W/mK at 300 K [2], which is higher than the value of 11 W/mK for $Y_3Al_5O_{12}$ (YAG) measured by the same method [3].

Sc_2O_3 (scandia) is isostructural to yttria and exhibits a thermal conductivity of 17 W/mK. The lattice constant of scandia is 9.79 Å. The Sc^{3+} ion is much smaller than the RE^{3+} dopant ions (RE = rare earth) causing a strong crystal field at the dopant site and a generally large Stark-splitting of the multiplets. Although the thermal conductivity is reduced in doped crystals in comparison to the undoped material, yttria and scandia are promising RE^{3+}-ion hosts for high power solid state lasers.

Due to the high melting points, about 2420°C, the growth of Y_2O_3 and Sc_2O_3 single crystals is rather difficult. Growth methods that have been established in the past include the Verneuil method [4], the flux method [5], the floating zone technique [6], and the laser heated pedestal growth method [7]. These techniques limit the size and optical quality of the crystals, which is the reason why yttria and scandia have not found widespread industrial application in the past. In a research program the synthesis of yttria and scandia crystals of rather good optical quality from the melt was demonstrated. Several RE-doped single crystals have been grown until now and were spectroscopically investigated. First laser results with samples doped with Nd^{3+}-, Yb^{3+}-, and Tm^{3+}-ions have been reported in Refs. [10–12]. In this paper we present spectroscopic data and laser parameters of Ho^{3+} and Er^{3+} doped crystals.

2. Crystal growth

The high melting points of yttria and scandia restrict the choice of crucible materials. The crucible has to be mechanically stable at the melting point of the oxide and must be resistant against chemical reactions with the melt as well as with the surrounding thermal insulation. Experiments with several crucible materials revealed that rhenium fulfills these requirements to the greatest extent. Rhenium is sensitive to oxidizing atmospheres

* Corresponding author. Tel.: +49-40-4283-85257; fax: +49-40-4283-86281.

E-mail address: petermann@physnet.uni-hamburg.de (K. Petermann)

0272-8842/00/$ - see front matter
PII: S0272-8842(99)00101-7

but resistant to melts of Al_2O_3 and RE oxides. The melting point of rhenium is 3180°C. During growth experiments the crucible was inductively heated with a power of approx. 20 kW at 230 kHz RF frequency. Because of the reactivity of the materials at high temperatures, any direct contact between the hot crucible and the ceramic zirconia insulation was avoided. A holding construction was designed which consisted of rhenium rods directly welded to the crucible. The crucible was suspended in a thermally insulating tube of zirconia felts so that it was completely surrounded by gas.

Cylindrical crucibles with a diameter of 20 mm and height of 25 mm were filled to about 75% with oxide melt. The crystals were grown in an inert helium atmosphere with a pulling rate of 1–3 mm/h and a rotation rate of 10 rpm. At the melting point the melt as well as the growing crystal appeared opaque in accordance with the comparatively high emissivity of the sesquioxides which was measured to be between 0.5 and 0.8 by McMahon [8]. The growth process itself was straight forward only for the first 2–5 mm of the growing crystal. Then the crystal lost contact with the melt or uncontrollable asymmetrical lateral growth started and the experiment had to be interrupted.

The problems with the diameter control are caused by a 'W'-shaped isotherm at the melt surface. At very high temperatures the heat transport is dominated by radiation according to the Stefan–Boltzmann law. The radiation power absorbed in the interface region of the growing crystal dissipates to the upper crystal surface mainly by heat conduction, because the radiative heat transport is inhibited by the opacity of the crystal. Due to the low heat conductivity of the crystaline material near the melting point, the temperature near the interface increases and becomes higher than at the uncovered surface of the melt around the crystal. When the heating power is reduced to maintain a constant crystal diameter, asymmetrical growth towards the cooler regions starts. We performed several experiments with different reflectors to reduce the radiation losses from the free melt surface. For this purpose rings and funnels were inserted into the crucible a few millimeters above the melt. However, larger crystals could not be obtained in this way until now.

3. Spectroscopic characteristics of Ho- and Er-doped crystals

Several crystals with typical length of 5 mm and diameter of 10 mm have been grown. The crystals show a brownish shade which vanishes after annealing in air at 1100°C for 48 h. We suppose that the brownish discoloration appears due to color centres caused by oxygen loss of the melt in accordance with the results of Berard et al. [9]. The annealed and polished crystals show mosaic structures and striations between crossed polarizers. The doped samples were spectroscopically investigated and tested for laser operation. Laser oscillation could be demonstrated in Tm: Y_2O_3 at 1950 nm [10], Yb: Sc_2O_3 at 1041 nm [11], Nd:Y_2O_3 at 1075 nm [12], as well as in Nd:Sc_2O_3 at various wavelengths [13]. Recently measurements were made on Ho and Er doped sesquioxides.

Ho^{3+}- and Er^{3+}-ions have shown laser action near 2 μm (Ho) and 3 μm (Er) in many hosts. These wavelengths are in the region of strong water absorption bands and therefore interesting for medical and eye-safe applications. Actually, one of the most efficient Ho-lasers emitting at 2 μm is Ho:YAG [14–16] and one of the best Er-lasers emitting near 3 μm is Er:YLF [17]. The absorption- and emission cross-section spectra of Ho:Sc_2O_3 and Er:Sc_2O_3 are shown in Figs. 1 and 2. The absorption spectra were measured with a spectrophotometer (Varian Cary 2400) and the fluorescence spectra with a FT-spectrometer (Biorad FTS 40). The emission cross-sections were determined with the method of McCumber [18] from the absorption cross-sections and with the Füchtbauer–Ladenburg equation [19] from fluorescence spectra. The spectra of RE^{3+}-ions in Y_2O_3 and Sc_2O_3 are similar. Some cross-sections and fluorescence lifetimes of Ho and Er doped samples are given in Table 1. The cross-sections of the 2.8 μm laser transition $^4I_{11/2} \rightarrow {}^4I_{13/2}$ in Er^{3+} have not been determined, because both levels involved in this transition

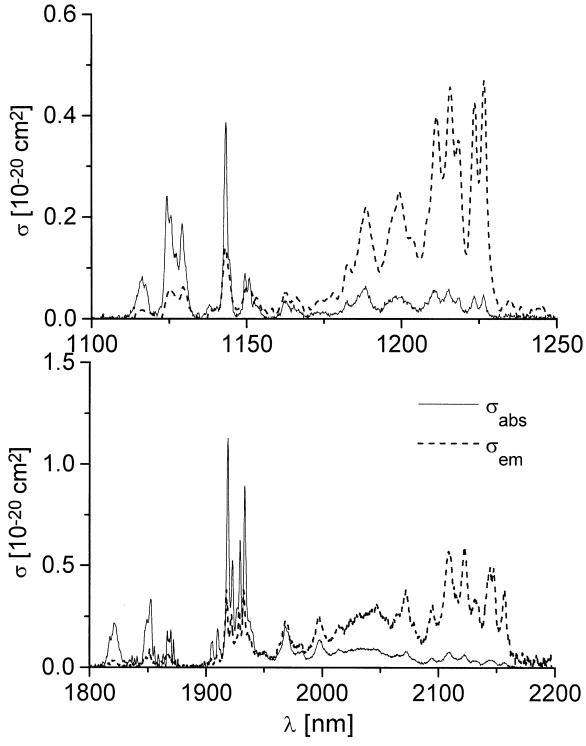

Fig. 1. Absorption and emission cross-sections of Ho:Sc_2O_3.

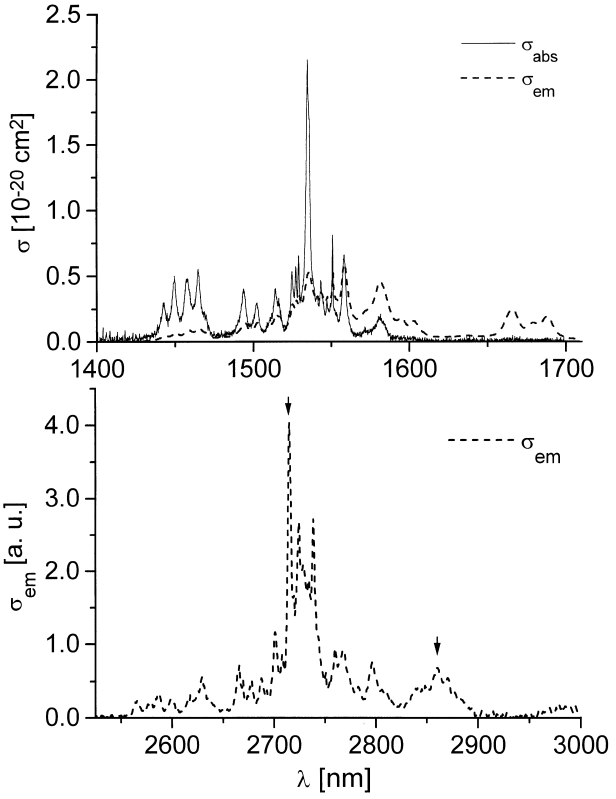

Fig. 2. Absorption and emission cross-sections of Er:Sc_2O_3. The arrows indicate the laser lines near 3 μm.

are metastable states and cross-sections have to be derived from excited state absorption (ESA) measurements.

The fluorescence decay curves after pulsed excitation show that the lifetimes of the $^4I_{13/2}$ manifold (lower laser level for 2.85 μm laser operation) and the $^4I_{11/2}$ manifold (upper laser level) in Er (1%): Y_2O_3 are very different. This causes self termination of the laser operation. At higher Er-concentrations the population dynamics change. Nonradiative interionic processes become important as described by Jensen et al. for Er:YLF [16]. The upper and lower laser level lifetimes are quenched and become comparable. At high excitation densities the lower laser level is depopulated by the upconversion process $^4I_{13/2}+{}^4I_{13/2}\rightarrow{}^4I_{9/2}+{}^4I_{15/2}$. The $^4I_{9/2}$ manifold population mainly decays into the upper laser level so that the population of the $^4I_{13/2}$ manifold is partly recycled for the laser process. Laser operation near 3 μm could be demonstrated in Er(2.3%): Sc_2O_3, which was the Sc_2O_3 sample with the highest Er-concentration available during the experiments. The crystal was placed near the flat mirror of a hemispherical resonator ($r_1=\infty$, $r_2=50$ mm) and was pumped with the focused beam of a laser diode providing up to 3.7 W pump power at 973 nm. Laser oscillation was achieved at 2715 and at 2816 nm in the quasi cw regime.

The output power was below 1 mW probably because the Er concentration is still too low. Y_2O_3 samples with higher Er^{3+} concentrations were also tested but no laser oscillation was observed due to the low crystal quality. A definite statement about the potential of Er-doped yttria and scandia crystals for 3 μm laser operation must therefore be postponed until samples of higher quality are available.

In Er:Sc_2O_3 and Er:Y_2O_3 fluorescence was also observed on the ground state transition $^4I_{13/2}\rightarrow{}^4I_{15/2}$ between 1650 and 1700 nm. This spectral region is interesting for eyesafe measuring systems. The reabsorption coefficient near 1.7 μm is very low due to the Stark splitting of 604 cm^{-1} of the Er $^4I_{13/2}$ ground state which is larger in Sc_2O_3 than in any other host. However, pump and probe measurements showed that the gain between 1630 and 1700 nm is considerably reduced by excited state absorption (ESA) from the $^4I_{13/2}$

Table 1
Spectroscopic parameters of Ho- and Er-doped yttria and scandia: absorption and emmission cross-sections as well as fluorescence lifetimes[a]

Crystal	Distribution coefficient	σ_{em} (10^{-21} cm^2) [@ wavelength (nm)]	σ_{abs} (10^{-21} cm^2) [@ wavelength (nm)]	τ (μs)
Ho(0.92%): Y_2O_3	0.93	4.1 (1216) 5.4 (2116) 3.1 (2127)	0.7 (1216) ≅0.6 (2116) ≅0.35 (2127)	1100 ($^4I_6$) 12 300 ($^4I_7$)
Ho(0.42%): Sc_2O_3	0.42	4.7 (1226.5) 4.9 (2148) 3.8 (2157)	0.47 (1226.5) 0.39 (2148) 0.26 (2157)	120 ($^4I_6$) 8560 ($^4I_7$)
Er(1%): Y_2O_3	1	1.54 (1661) Not calibrated at 2800 nm	≅0.2 (1661) ESA from $^4I_{13/2}$	11 000 ($^4I_{13/2}$) 2760 ($^4I_{11/2}$)
Er(9.5%): Y_2O_3				1600 ($^4I_{13/2}$) 1250 ($^4I_{11/2}$)
Er(2.3%) Sc_2O_3	0.41	1.92 (1688) Not calibrated at 2800 nm	≅0.15 (1688) ESA from $^4I_{13/2}$	8500 ($^4I_{13/2}$) 310 ($^4I_{11/12}$)

[a] The lifetimes were measured with high excitation densities. The concentrations refer to the doped cation sites.

Table 2
Ratio between absorption and emission cross-sections in Ho-doped crystals

	Ho:Y_2O_3	Ho:Sc_2O_3	Ho:YAG
σ_{em}/σ_{abs}	9 @ 2116 nm 9 @ 2127 nm	12.5 @ 2148 nm 14.5 @ 2157 nm	4.45 @ 2090 nm 6.88 @ 2122 nm

manifold into the $^4I_{9/2}$ multiplet. For this reason stimulated emission is only expected in Er:Sc_2O_3 in a small region near 1680 nm with an effective cross-section of 1.4×10^{-21} cm^2. In Er:Y_2O_3 amplification of radiation on the ground state transition is completely impossible due to ESA.

Although Ho-doped Y_2O_3 or Sc_2O_3 samples were not tested for laser oscillation, the spectroscopic data are very promising. The emission cross-sections in the region of low absorption are smaller than in Ho:YAG where the peak emission cross-sections are 9.8×10^{-21} cm^2 at 2090 nm and 5.5×10^{-21} cm^2 at 2122 nm. However, the ratios between emission and absorption cross-sections which are also important for the laser threshold are much better in Ho:Y_2O_3 and Ho:Sc_2O_3. Ho:Sc_2O_3, in particular, exhibits low reabsorption losses because of the large Stark-splitting of the Ho ground state manifold $^5I_8$. The values σ_{em}/σ_{abs} near 2150 nm are summarized in Table 2.

Besides the emission near 2 μm, the Ho-doped Y_2O_3 and Sc_2O_3 crystals show an interesting fluorescence around 1.2 μm (Fig. 1). Few lasers have been realized in this wavelength region. Codoping is necessary if diodes are used as pumping sources. Ho lasers emitting at 2 μm are often codoped with Tm^{3+}-ions which show an absorption band near 800 nm. For Ho lasers operating near 1.2 μm Yb^{3+} is a favourable codopant. The Yb^{3+}-ions absorb efficiently the emission of InGaAs diodes near 970 nm and transfer the pump energy to the Ho $^5I_6$ upper laser multiplet. Laser tests of Ho-doped sesquioxide crystals codoped with Tm and Yb are planned for 2 μm as well as for 1.2 μm operation.

4. Summary

We have grown several lanthanide-doped yttria and scandia crystals by the Czochralski method. The thermal properties of these materials at their melting points and the strong radiation from the melt at 2500°C seem to inhibit the production of large crystal boules by the conventional Czochralski method.

Recently large crystal boules of 40 mm diameter and 20 mm height have been grown from rhenium crucibles by the Bridgman technique; single crystals of about 1 cm^3 volume could be prepared.

First spectroscopic investigations and laser tests of a variety of lanthanide-doped yttria and scandia crystals revealed the potential of these materials. Effective emission cross-sections of the Ho^{3+}-ion are 3.1×10^{-21} cm^2 @ 2127 nm in Y_2O_3 and 3.8×10^{-21} cm^2 @ 2157 nm in Sc_2O_3. For pumping of the Ho^{3+}-ions with laser diodes Yb- or Tm-codopants are needed.

Er:Sc_2O_3 shows stimulated emission near 2.8 μm. A much higher laser efficiency can be predicted for samples with an improved optical quality. Especially Er-doped Y_2O_3 crystals of higher perfection should show laser operation near 3 μm because they combine a long lifetime of the upper laser level $^4I_{11/2}$ with an upconversion that depopulates the lower laser level $^4I_{13/2}$ and recycles population for the laser process.

Acknowledgements

This work was funded by the German Bundesministerium für Bildung, Wissenschaft, Forschung und Technologie (BMBF) under the project number 13N6749-2. We wish to thank Mrs. B. Cornelisen for the microprobe analyses.

References

[1] L. Pauling, M.D. Shappell, Z. Krist. 75 (1930) 128.
[2] Measurements by the pulse method at the Austrian Research Centers, Seibersdorf.
[3] K. Contag, Measurements by the pulse method at the Austrian Research Centers, Seibersdorf.
[4] C. Bartá, F. Petru, B. Hájek, Die Naturwissenschaften 45 (1957) 36.
[5] C. Changkang, B.M. Wanklyn, P. Ramasamy, J. Cryst. Gr. 104 (1990) 672.
[6] D.B. Gasson, D.S. Cockayne, J. Mater. Sci. 5 (1970) 100.
[7] B.M. Tissue, L. Lu, L. Ma, W. Jia, M.L. Norton, W.M. Yen, J. Cryst. Gr. 109 (1991) 323.
[8] W.R. McMahon, D.R. Wilder, J. Am. Ceram. Soc. 51 (1968) 188.
[9] M.F. Berard, C.D. Wirkus, D.R. Wilder, J. Am. Ceram. Soc. 51 (1968) 644.
[10] A. Diening, B.-M. Dicks, E. Heumann, J.-P. Meyn, K. Petermann, G. Huber, in: C.R. Pollock and W.R. Bosenberg (Eds.) OSA Trends in Optics and Photonics, Vol. 10, Advanced Solid-State Lasers, Optical Society of America, Washington DC, 1997, p. 194.
[11] E. Mix, L. Fornasiero, A. Diening, K. Petermann, G. Huber, Advanced Solid-State Lasers, Technical Digest, Optical Society of America, Washington DC, 1998 p. 258.
[12] V. Peters, L. Fornasiero, E. Mix, A. Diening, K. Petermann, Verhandl, DPG (VI) 33 (1998) 206(Q 41.4).
[13] L. Fornasiero, E. Mix, V. Peters, E. Heumann, K. Petermann, G. Huber, Advanced Solid-State Lasers, Technical Digest, Optical Society of America, Washington DC, 1999 p. 88–90.
[14] M. Falconeri, A. Lanzi, G. Silvetti, Appl. Phys. B 62 (1995) 537.
[15] C.D. Nabors, J. Ochoa, T.Y. Fan, A. Sanchez, H.K. Choi, G.W. Turner, IEEE J. Quant. Electr. 31 (9) (1995) 1603.
[16] B.M. Dicks, Diploma thesis, Hamburg, 1997.
[17] T. Jensen, A. Diening, G. Huber, B.H.T. Chai, Opt. Lett. 21 (1996) 585.
[18] D.E. McCumber, Phys. Rev 136 (4A) (1964) 954.
[19] L. DeLoach, S.A. Payne, L.L. Chase, L.K. Smith, K.W. Kway, W.F. Krupke, IEEE J. Quant. Electr. 29 (4) (1993) 1179.